Carriers Transport in Quantum Dot Quantum Well Microstructures of Self-assembled CdTe/CdS/Ligand Core-shell System

Kuiying Li*, Wenling Shi, Qiuxia Li, Wenke Ma

State Key Laboratory of Metastable Materials Manufacture Technology & Science, Yanshan University, Qinhuangdao 066004, China
* Corresponding author, E-mail addrass: kuiyingli@ysu.edu.cn

ABSTRACT

Surface photovoltaic (SPV) technique was used for probing the fine electron structures and charge transport characteristics in the quantum dots (QDs). A super-atom system of the ligand-stabilized CdTe nanoparticles upon illumined by UV-NIR light, which was composed of the core of $CdTe_{1-x}S_x$ ($0 \le x \le 1$) ultra-fine nanoparticles and the external surface capped by the cluster of some ligand, was experimental confirmed. A quantum dot quantum well (QDQW)'s graded-band-gap structure existed in the system, and resonance quantum tunneling in the QDQWs depended strongly on the properties of the ligands, because the depth of the QWs buried in different interface SCRs was closely related to the molecular conformation of the ligand according to the SPV measurements. If more S atom in -HS group of the ligands participated in forming the $CdTe_{1-x}S_x$ ($0 < x < 1$) layer in between the core-CdTe and the ligands, it might cause an obvious resonance quantum tunneling in the QDQW structure, prolong the photo-generation free charge carrier's (FCC's) lifetime at illumination of photonic energy $h\upsilon \ge E_{g,\ core\text{-}CdTe}$.

Keywords: CdTe nanocrystal, core-sheel structure, quantum dot quantum well, photogenic carriers, surface photovoltage spectroscopy

1 INTRODUCTION

In the last decade, there has been a steady increase in theoretical research and experimental work on various core-shell structure semiconductor nanocrystals to be related as QDs. [1, 2]These have been carried out by means of various research methods. [3-5]The interest in these nanostructures is due to their unique electrical, optical, and transport characteristics as compared with conventional materials, even two- and one-dimensional nanomaterials. [6, 7] The electron energy levels and resonance quantum tunnel effect of the QWs that were buried in super-lattice structures have the potential for widespread use in the fields of advanced generation photoelectronic and microelectronic devices. [8-10] Research into one particular high-quality QD consisting of II/VI semiconductors, a ligand-stabilized CdTe QD, has recently excited interest because of the quantum confinement effect, and because of its widespread use as biomarkers, luminescent materials, and photon crystals. [11-13] Research into the QDs has mainly focused on synthetic methods, morphology, electronic and optical properties.[14-17] The study of charge transport behaviors in the QDQWs microstructure of the self-assembled CdTe/CdS/ligand nanoparticles, however, has rarely been reported so far. In our previous studies, [18, 19] SPV technique has been used to probe the characteristic charge transfer transition channels on the surfaces and at buried interfaces for different ligand-capped crystalline CdTe nanoparticles. This behavior is closely related to the energy transformation among specific quantum states, such as the electron and vibration levels of an elementary reaction. In order to carry out a microscopic study of possible charge transport mechanisms in the QDQWs' structure that is formed in between the ligand and the CdTe nanoparticles in terms of the self-assembled core-shell nanostructure, in the present paper, the microstructure of the QDQWs and the photo-generated FCC's transport behaviors in CdTe nanoparticles capped by various ligands were studied by SPV technology.

2 EXPERIMENTAL

The samples prepared were denoted as MPA-r, MA-r, TGA-r, and TG-r, where 3-mercaptopropionic acid (MPA), β-mercaptoethylamine (MA), thioglycolic acid (TGA), and 1-thioglycerol (TG); -r indicated MPA (MA, TGA, or TG) -capped CdTe nanoparticles with an average particle size of 4.0 nm (red). High-resolution transmission electron micrographs (HRTEM) and fast Fourier transform (FFT) were recorded on a JEOL-2010 electron microscope (Japan) operating at 200 kV. Fourier transform infrared spectroscopy (FTIR) was recorded on a Bruker EQUINOX55 FTIR (Germany). The principles and experimental details of SPV spectroscopy have been described elsewhere. [20, 21]

3 EXPERIMENTAL RESULTS AND DISCUSSION

3.1 Clarification of a super-atom structure of ligand-capped CdTe nanoparticles

The HRTEM and FFT of the sample MPA-r are shown in Fig.1a: the interplanar spacings of selected nanocrystalline grains were 0.341 nm, 0.336 nm, and 0.339 nm, respectively. All three values were between the interplanar spacings of the (111) planes of the CdTe and CdS lattices. However, the cell parameter was closer to that of CdTe with a sphalerite structure according to the electron diffraction pattern and the indexing analysis. This implies that a distortion of the lattice cell occurred because sulfur atoms in the ligand MPA partially replaced tellurium atoms located at the surfaces and the boundary of CdTe nanoparticles. Energy-dispersive X-ray spectroscopy (EDS) of the samples MPA-r and TGA-r (Figs. 1b and 1c) also indicated that the samples consisted essentially of Cd, Te, and S elements, resulting from the -HS group in the ligands coordinating with CdTe nanoparticles, i.e. the S atoms in the group may partially replace Te atoms located on the surface and grain boundary of CdTe nanoparticles, and then form a CdS layer capped on the surface of the nanoparticles. In addition, the relative contents of S atoms and Cd or Te atoms in the MPA sample were about twice that in the TGA sample as seen in Figs. 1b and 1c.

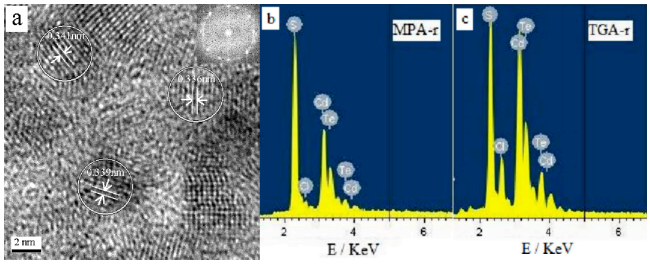

FIG. 1. High-resolution transmission electron micrographs and fast Fourier transform of the sample MPA-r (a); energy dispersive X-ray spectra of MPA (b) and TGA (c)-capped CdTe nanoparticles.

Figure 2 shows the FTIR spectra of the samples MPA-r, MA-r, TGA-r, and TG-r. According to a spectra library the broad and strong absorption peak at 3394 cm^{-1} was assigned to the -OH vibration at alkyl chains in some ligand, υ_{-OH}. For MPA- and TGA-stabilized CdTe nanoparticles, two narrow absorption peaks at 1386 and 1590 cm^{-1} were assigned to the COO- stretching vibration, υ_{COO-}, and the C=O stretching vibration, $\upsilon_{C=O}$, respectively. It is significant that the absorption peak that was associated with the S-H stretching vibration, υ_{S-H}, disappeared at 2550 cm^{-1} for all four samples. This implies that the S-H bond in those ligands had been broken, and that then the Cd-S bond may be made in the self-assembly process of the core-shell structural nanoparticles. These deductions were consistent with the HRTEM and EDS results of the samples MPA-r and TGA-r shown in Fig. 1. The core-shell system at illumined by UV-NIR light may be called "super-atom structures" according to the definition[22] and to the experimental results shown in the present paper. More specifically, it can be assumed that the core of the super-atom is a $CdTe_{1-x}S_x$ ultra-fine particle with an average grain size of 4 nm, which can be a donor or an acceptor according to the magnitude of the electron affinity of the core-CdTe. The external surface of the grain may be capped by the cluster of some ligand that was incorporated in the $CdTe_{1-x}S_x$ ultra-fine particle by breaking the S-H bond and then making the Cd-S bond.

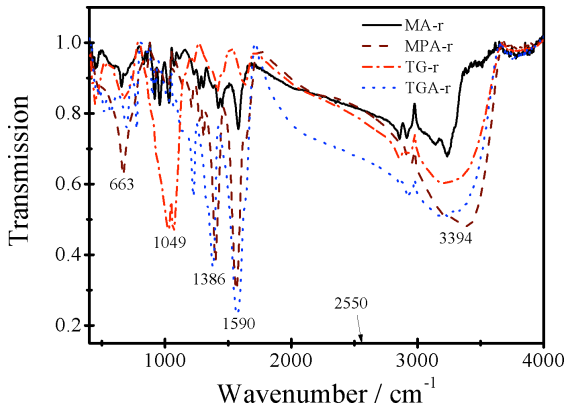

FIG. 2. Fourier transform infrared spectra of the samples MPA-r, MA-r, TGA-r, and TG-r.

3.2 Analysis of surface photovoltaic spectroscopy

The SPV spectra of the samples MPA-r, MA-r, TGA-r, and TG-r are shown in Figs. 3a, 3b, 3c, and 3d, respectively. The inset in Fig. 3b shows our setup for SPV spectroscopy. In the SPV spectra of all four samples, there appeared three SPV response peaks, $knee_1$, $knee_2$, and $knee_3$, and two valleys, QW_1 and QW_2, in the wavelength range of UV-NIR light. It is interesting that the four samples varied from one another in both the intensity of the SPV response and the photon energy resulting in the charge transfer transitions, corresponding to these peaks and valleys in Figs. 3a, 3b, 3c, and 3d. Obviously, these were caused by the different ligands used. In the previous report,[18] the three SPV response peaks related to the $knee_1$, $knee_2$, and $knee_3$ were assigned to the photo-generated FCC's transfer transitions, and were connected with the optical bandgaps of $E_{g,\ core\text{-}CdTe}$, $E_{g,\ shell\text{-}CdS}$, and $E_{g,\ outer\text{-}layer\text{-}ligand}$, respectively, according to the abscissa of the largest external tangent of the band, the calculated photoelectric thresholds of the SPV responses. The two valleys of the SPV response of the four samples were attributed to the photo-generated charge transfer transitions in connection with the two quantum wall structures QW_1 and QW_2, which were respectively located in the interface SCR_1 between the core-CdTe and the shell-CdS, and SCR_2 between the shell-CdS and some ligand of the ligand-capped CdTe super-atom structure as indicated in Fig. 4a. This was because in between those three 'knees', the shape

of the SPV spectrum resembles (an inverted) typical absorption spectra of multi-quantum-well (MQW) structure. [23] The photon energies associated with the two QWs in Fig. 3 were denoted as E_{QW1} and E_{QW2}, respectively. Evidently, the properties of the ligands may directly affect the depth of the QWs in the super-atom structure. The graded-band-gap scheme of the super-atom structure of the samples are illustrated in Fig. 4b, according to the numerical value of the photon energies that were related to the knees and valleys of the SPS of the four samples in Fig. 3.

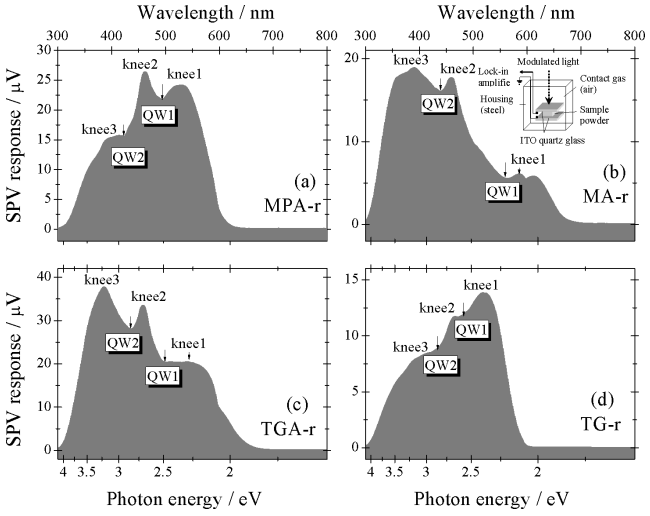

FIG. 3. Surface photovoltaic spectra of the samples MPA-r (a), MA-r (b), TGA-r (c), and TG-r (d). The inset in (b) shows our setup for SPV spectroscopy.

TABLE 1. The quantum well parameters obtained by the results of surface photovoltaic spectroscopy of the samples.

Quantum well parameter*/eV \ Sample	MPA-r	MA-r	TGA-r	TG-r
$E_{g,core\text{-}CdTe}$	2.35	2.12	2.38	2.39
$E_{g,shell\text{-}CdS}$	2.69	2.69	2.69	2.69
$E_{g,outer\text{-}layer\text{-}ligand}$	3.12	3.17	3.22	3.04
E_{QW1}	2.51	2.20	2.49	2.54
E_{QW2}	2.92	2.81	2.85	2.86
ΔE_{C1}	0.16	0.08	0.11	0.15
$\mathbf{\Delta E_{C2}}$	0.23	0.12	0.16	0.17

* $E_{g,\ core\text{-}CdT}$, $E_{g,\ shell\text{-}CdS}$, and $E_{g,\ outer\text{-}layer\text{-}ligand}$ represent the band-gaps related to the core-CdTe, the shell-CdS, and the outer-layer-ligand, respectively; E_{QW1} and E_{QW2} denote the photon energies associated with the QW_1 and QW_2, respectively; $\Delta E_{C1} = E_{QW1} - E_{g,\ CdTe}$; $\Delta E_{C2} = E_{QW2} - E_{g,\ CdS}$.

In comparing the d-value $\Delta E_{C1\ or\ 2}$ of the four samples in Table 1, an interesting order can be seen: $\Delta E_{C1\ or\ 2,\ MPA\text{-}r} > \Delta E_{C1\ or\ 2,\ TG\text{-}r} > \Delta E_{C1\ or\ 2,\ TGA\text{-}r} > \Delta E_{C1\ or\ 2,\ MA\text{-}r}$. According to the literature[24, 25] the QWs in a semiconductor heterostructure may result in resonance quantum tunneling, and the deeper the QWs in its energy band, the more obvious is the resonance quantum tunneling, when the width of the QWs is so thin as to cause a strong coupling between the QWs. If we do not think resonance quantum tunneling in the system, the situation can be that the FCCs carrying with negative charge in a sample, which were induced by illumination with the photon energy $h\upsilon \geq E_{g,\ outer\text{-}layer\text{-}ligand}$, moved from the outer-layer-ligand to the core-CdTe; the holes may be partially trapped in the QW_1 and QW_2 that were located at the interfaces SCR_1 and SCR_2, respectively, because the electron affinity of the core-CdTe was greater than that of the outer-layer-ligand as shown in the middle of Fig. 4. Consequently, obvious resonance quantum tunneling should contribute to increase in those photo-generated FCCs' diffusion lengths upon illuminated by the photon energy $h\upsilon \geq E_{g,\ core\text{-}CdTe}$, and to enhance the SPV characteristics of the core-CdTe in the core-shell structure nanoparticles, because of the fact that the potential well depths $\Delta E_{C1\ or\ 2,\ MPA}$ and $\Delta E_{C1\ or\ 2,\ TG}$ of the samples MPA-r and TG-r were deeper than that of the samples MA-r and TGA-r. The experimental results above prove these theoretical deductions[26]. Furthermore, considering the possible core-shell structure of the four samples, the coordinate bond may be formed between the lone-pair electrons of the carbonyl or amido group at the alkyl chain of some ligand and the unoccupied s-orbital of the Cd^{2+} ions located at the surface of CdTe nanoparticles. At the same time the S atom in -HS group of the ligands may partially replace the Te atom in CdTe, and then form a CdS layer capped on the surface of CdTe nanoparticles. Other unbonded lone-pair electrons in the ligand, such as that in amido groups of the ligand MA and in hydroxyl groups of the ligand TGA, can be excited to the π antibonding orbital of the ligand upon illumination by photon energy $h\upsilon \geq E_{g,\ outer\text{-}layer\text{-}ligand}$, which is the so-called n-π^* transition. The n-π^* transition occurring within the ligand may have an inhibiting effect on resonance quantum tunneling.

As compared $knee_1$s in Fig. 3 of the samples MA-r and TGA-r with the samples MPA-r and TG-r, the SPV response zone of $knee_1$ of the first two had an obvious broadening to longer wavelength, even appeared twinned peaks in 575 nm to 625 nm as the situation of the sample MA-r shown in Fig. 3b. The reason leading to the broadened and twinned peaks of $knee_1$ of the samples MA-r and TGA-r in Figs. 3b and 3c may be attributed to those photo-generation FCC's transfer transitions between surface states that were some dangling bonds and the energy band, because S-atoms in the ligands MA and TGA, which can bonded with the dangling bonds at the surface and grain boundary of the two samples, were less than that of the samples MPA-r and TG-r as the typical results displayed in Figs. 1b and 1c. The above situation of the samples MPA-r and TG-r may become more obvious, because more S atom in -HS group of the ligands MPA and TG participated in forming the $CdTe_{1-x}S_x$ layer as

compared with the samples MA-r and TGA-r, causing the stronger SPV response of knee$_1$ than that of knee$_3$ in terms of the samples MPA-r and TG-r as seen in Figs. 3a and 3d. On the contrary, a weak resonance quantum tunneling in the QDQW's structure resulted in the broadened and twinned peaks of knee$_1$ at the long wavelength region of the samples MA-r and TGA-r as shown in Figs. 3b and 3c, due to less S-atoms in -HS group of the ligands MA and TGA participated in bonding with the dangling bonds at the surface and grain boundary of the core-CdTe.

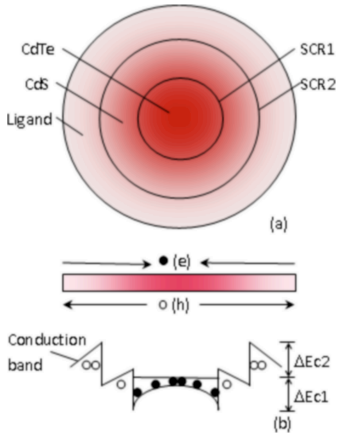

FIG. 4. Super-atom scheme models at illumination of UV-NIR light (a) and graded-band-gap of self-assembled CdTe/CdS/ligand core-shell structure (b), in which the values of ΔE_{C1} and ΔE_{C2} refer to Table 1.

4. CONCLUSION

A super-atom system of the ligand-stabilized CdTe nanoparticles was experimental confirmed, which was composed of the core of $CdTe_{1-x}S_x$ ($0 \leq x \leq 1$) ultra-fine nanoparticles with an accepter characteristic at illumination of UV-NIR light and the external surface capped by the cluster of some ligand. According to the SPV characteristics of the QDs, a QDQW's structure with graded-band-gap existed in the system, and the resonance quantum tunneling in the QDQWs depended strongly on the properties of the ligands. More specifically, if more S atom in -HS group of the ligands participated in forming the $CdTe_{1-x}S_x$ ($0 < x < 1$) layer in between the core-CdTe and the ligands, it would cause an obvious resonance quantum tunneling in the QDQWs, which might prolong the photo-generation FCC's lifetime at illumination of photonic energy $h\upsilon \geq E_{g,\ core\text{-}CdTe}$, and at the same time decrease the number of the surface states that were related to the non-radiative de-excitation processes upon illumination especially by the photonic energy $h\upsilon < 2.1$ eV.

REFERENCES

[1] B. Bochorishvili, Physica E: Low-dimensional Systems and Nanostructures **43**, 874, 2011.

[2] P. K. Santra, R. Viswanatha, S. M. Daniels, N. L. Pickett, and J. M. Smith, P. O'Brien, and D. D. Sarma, J. Am. Chem. Soc. **131**, 470, 2009.

[3] A. Khaetskii, V. N. Golovach, X. Hu, and I. Žutić , Phys. Rev. Lett. **111**, 186601, 2013.

[4] A. Mews, A. Eychmueller, M. Giersig, D. Schooss, and H. Weller, J. Phys. Chem. **98,** 934, 1994.

[5] A. Mews, A. V. Kadavanich, U. Banin, and A. P. Alivisatos, Phys. Rev. B **53,** 13242, 1996**.**

[6] Y. N. Fang, M. Xiao and D. Z. Yao, Physica E: Low-dimensional Systems and Nanostructures **42**, 2178, 2010.

[7] L. Esaki and R. Tsu, IBM Research Note RC-2418 (1969). IBM J. Res. Develop. **14**, 61, 1970.

[8] D. Guzun, Yu. I. Mazur, V. G. Dorogan, M.E. Ware, J. Appl. Phys. **113**, 154304-5, 2013.

[9] R. Dingle, W. Wiegmannn, and C. H. Herny, Phys. Rev. Lett. **33,** 824, 1974.

[10] R. Kostić and D. Stojanović, Acta Phys. Pol. A **116,** 598, 2009.

[11] A. M Smith, S. Dave, S. Nie, L. True, and X. Gao, Expert Rev. Mol. Dtagn. **6,** 231, 2006.

[12] S. J. Cho, D. Maysinger, M. Jain, B. Röder, S. Hackbarth, and F. M. Winnik, Langmuir **23,** 1974, 2007.

[13] J. Y. Zhang, X. Y. Wang, and M. Xiao, Opt. Lett. **28,** 1430, 2003.

[14] A. L. Rogach, L. Katsikas, A. Kornowski, D. Su, A. Eychmüller, and H. Weller, Ber Runsenges. Phys. Chem. **100**, 1772, 1996.

[15] A. V. Nashchekin, K. G. Kolmakov, I. P. Soshnikov, N. M. Shmidt, and A. V. Loskutov, Tech. Phys. Lett. **29**, 575, 2003.

[16] A. L. Rogach, L. Katsikas, A. Kornowski, D. Su, A. Eychmüller, and H. Weller, Ber Runsenges. Phys. Chem. **101**, 1668, 1997.

[17] H. Zhang and B. Yang, Thin Solid Films **418,** 169, 2002.

[18] K. Y. Li, H. Zhang, W. Y. Yang, S. L. Wei, and D. Y. Wang, Mate. Chem. Phys. **123**, 98, 2010.

[19] K. Y. Li, G. J. Song, J. Zhang, C. M. Wang, and B. Guo, J. Photochem. Photobiol. A **218**, 213, 2011.

[20] L. Kronik and Y. Shapira, Surf. Sci. Rep. **37,** 1-206, 1999.

[21] A. Rosencwaig, Science **181,** 657, 1973.

[22] T. Inoshita, S. Ohnishi and A. Oshiyama, Phys. Rev. Lett. **57,** 2560, 1986.

[23] D. Gal, et al., AIP Conf. Proc. **353,** 453, 1996.

[24] S. Yuasa, T. Nagahama, and Y. Suzuki, Science **297,** 234, 2002.

[25] T. Niizeki, N. Tezuka, and K. Inomata, Phys Rev Lett. **100,** 047207, 2008.

[26] P. Harrison, "Quantum wells, wires and dots theoretical and computational physics of

semiconductor nanostructures", Second Edition, John Wiley & Sons, Ltd, 285, 2005.